

Plasma microRNA signature associated with skeletal muscle wasting in post-menopausal osteoporotic women

Martina Faraldi^{1*}, Veronica Sansoni¹, Jacopo Vitale², Silvia Perego¹, Marta Gomasca¹, Chiara Verdelli³, Carmelo Messina^{4,5}, Luca M. Sconfienza^{4,5}, Giuseppe Banfi^{1,6}, Sabrina Corbetta^{7,8} & Giovanni Lombardi^{1,9}

¹Laboratory of Experimental Biochemistry and Molecular Biology, IRCCS Istituto Ortopedico Galeazzi, Milan, Italy; ²Laboratory of Movement and Sport Science, IRCCS Istituto Ortopedico Galeazzi, Milan, Italy; ³Laboratory of Experimental Endocrinology, IRCCS Istituto Ortopedico Galeazzi, Milan, Italy; ⁴OU Diagnostic and Interventional Radiology, IRCCS Istituto Ortopedico Galeazzi, Milan, Italy; ⁵Department of Biomedical Science for Health, University of Milan, Milan, Italy; ⁶Vita-Salute San Raffaele University, Milan, Italy; ⁷Department of Biomedical, Surgical and Dental Sciences, University of Milan, Milan, Italy; ⁸Endocrinology and Diabetology Service, IRCCS Istituto Ortopedico Galeazzi, Milan, Italy; ⁹Department of Athletics, Strength and Conditioning, Poznań University of Physical Education, Poznań, Poland

Abstract

Background Skeletal muscle mass wasting almost invariably accompanies bone loss in elderly, and the coexistence of these two conditions depends on the tight endocrine crosstalk existing between the two organs, other than the biomechanical coupling. Since the current diagnostics limitation in this field, and given the progressive population aging, more effective tools are needed. The aim of this study was to identify circulating microRNAs (miRNAs) as potential biomarkers for muscle mass wasting in post-menopausal osteoporotic women.

Methods One hundred seventy-nine miRNAs were assayed by quantitative real-time polymerase chain reaction in plasma samples from 28 otherwise healthy post-menopausal osteoporotic women (73.4 ± 6.6 years old). The cohort was divided in tertiles based on appendicular skeletal muscle mass index (ASMMI) to better highlight the differences on skeletal muscle mass (first tertile: $n = 9$, ASMMI = $4.88 \pm 0.40 \text{ kg}\cdot\text{m}^{-2}$; second tertile: $n = 10$, ASMMI = $5.73 \pm 0.23 \text{ kg}\cdot\text{m}^{-2}$; third tertile: $n = 9$, ASMMI = $6.40 \pm 0.22 \text{ kg}\cdot\text{m}^{-2}$). Receiver operating characteristic (ROC) curves were calculated to estimate the diagnostic potential of miRNAs. miRNAs displaying a statistically significant fold change $\geq \pm 1.5$ and area under the curve (AUC) > 0.800 ($P < 0.05$) between the first and third tertiles were considered. A linear regression model was applied to estimate the association between miRNA expression and ASMMI in the whole population, adjusting for body mass index, age, total fat (measured by total-body dual-energy X-ray absorptiometry [DXA]) and bone mineral density (measured by femur DXA). Circulating levels of adipo-myokines were evaluated by bead-based immunofluorescent assays and enzyme-linked immunosorbent assays.

Results Five miRNAs (hsa-miR-221-3p, hsa-miR-374b-5p, hsa-miR-146a-5p, hsa-miR-126-5p and hsa-miR-425-5p) resulted down-regulated and two miRNAs (hsa-miR-145-5p and hsa-miR-25-3p) were up-regulated in the first tertile (relative-low ASMMI) compared with the third tertile (relative-high ASMMI) (fold change $\geq \pm 1.5$; P -value < 0.05). All the corresponding ROC curves had AUC > 0.8 ($P < 0.05$). Two signatures hsa-miR-126-5p, hsa-miR-146a-5p and hsa-miR-425-5p; and hsa-miR-126-5p, hsa-miR-146a-5p, hsa-miR-145-5p and hsa-miR-25-3p showed the highest AUC, 0.914 (sensitivity = 77.78%; specificity = 100.00%) and 0.901 (sensitivity = 88.89%; specificity = 100.00%), respectively.

Conclusions In this study, we identified, for the first time, two miRNA signatures, hsa-miR-126-5p, hsa-miR-146a-5p and hsa-miR-425-5p; and hsa-miR-126-5p, hsa-miR-146a-5p, hsa-miR-145-5p and hsa-miR-25-3p, specifically associated with muscle mass wasting in post-menopausal osteoporotic women.

Keywords osteoporosis; plasma miRNAs; plasma myokines; sarcopenia

Received: 18 January 2023; Revised: 7 November 2023; Accepted: 7 December 2023

*Correspondence to: Martina Faraldi, Laboratory of Experimental Biochemistry and Molecular Biology, IRCCS Istituto Ortopedico Galeazzi, Milan, Italy.

Email: martina.faraldi@grupposandonato.it

Martina Faraldi and Veronica Sansoni have contributed equally to the study.

Introduction

Osteoporosis and sarcopenia are disorders that predominantly occur in elderly people: osteoporosis is characterized by decrease bone mineral density (BMD), increase bone fragility and fracture risk, while sarcopenia is characterized by decrease muscle mass, impaired muscle function and increase risk of fall.^{1,2} Muscle and bone form a functional unit that, besides the mechanical coupling, relies on a two-way endocrine-like signalling that sees several soluble mediators produced in one tissue, in response to specific stimuli, acting on the other. Every impairment of this finely tuned crosstalk leads to dysfunctions in both tissues. For these reasons, conditions of impaired bone quality and strength, for example, osteopenia and osteoporosis, and conditions of muscle mass wasting and impaired muscle strength, for example, sarcopenia, often coexist and hesitate into an increasingly discussed multifactorial syndrome called osteosarcopenia featured by significant worsened outcomes than those observed in any single condition.³ With the increased life expectancy and population aging, this condition is going to increase, as well as the associated outcomes like increased risk of falls, higher incidence of fractures, impaired mobility and disability, fragility, hospitalization and mortality, and, nonetheless, to the increase of healthcare costs.

Until now, a unique and standardized diagnostic method for osteosarcopenia has not been introduced into clinical practice. Osteosarcopenia diagnosis is based, indeed, on the combination of osteoporosis and sarcopenia criteria. Dual-energy X-ray absorptiometry (DXA) is recommended for BMD measurement: the World Health Organization has defined as osteoporotic those people who show a BMD *T*-score < -2.5, at any site.⁴ Sarcopenia diagnosis, instead, takes into account skeletal muscle mass and function measurement: DXA and bioelectrical impedance analysis (BIA) are used for skeletal muscle mass measurement, while grip strength and gait speed to assess skeletal muscle mass strength and function.⁵ For both osteoporosis and sarcopenia, tools to evaluate the risk of adverse outcomes, such as FRAX (prediction of the 10-year risk of hip fractures)⁶ and SARC-F (five-item questionnaire to evaluate sarcopenia risk),⁷ have been validated into clinical practice while neither rapid tests nor screening to either predict osteosarcopenia or assess any potential risk associated with the condition exists. Therefore, predictive and diagnostic methods to early diagnose bone and skeletal muscle loss should be implemented into clinical practice. The assessment of bone and skeletal muscle cells metabolism, through the measurement of circulating biomarkers, such as C-terminal cross-linked telopeptide (CTX-I), osteocalcin (OC), tartrate-resistant acid phosphatase-5b (TRAP5b), bone alkaline phosphatase (BALP)

and insulin-like growth factor (IGF-1), has been suggested to support the early diagnosis of osteosarcopenia.^{8,9} However, as known, these markers suffer of several limitations and, among these, the most relevant one is the lack of any marker specific for the combination of bone and muscle wasting in the elderly. Circulating microRNAs (miRNAs) may represent a promising alternative. miRNAs are small non-coding RNA involved in the post-transcriptional regulation of gene expression.¹⁰ miRNAs are expressed by almost all tissues where they play important roles in multiple biological processes (BPs), including bone and skeletal muscle homeostasis.¹¹ miRNAs can also be secreted, in response to both physiological and pathological stimuli, into body fluids in a stable form, associated with proteins or encapsulated into extracellular vesicles. Being stable, easily detectable and sensitive to changes in the physiological status, circulating miRNAs could represent optimal non-invasive biomarkers to monitor pathophysiological processes, with diagnostic and prognostic potential. Several studies investigated the role of circulating miRNAs as diagnostic biomarkers in different disorders (i.e., cancer and Alzheimer).¹²

It has been demonstrated that alterations in miRNA transcription levels or miRNA circulating levels are associated to the development and progression of either skeletal muscle or bone diseases that occur during aging, as sarcopenia and osteoporosis.^{11,13}

He and colleagues have identified six miRNAs (miR-155, miR-208b, miR-222, miR-210, miR-328 and miR-499) significantly down-regulated in sarcopenic patients compared with healthy elderly and significantly associated with diagnostic indexes of sarcopenia.¹⁴ Differentially expressed circulating miRNAs have been also observed in osteoporotic and non-osteoporotic patients suggesting their use in clinical routine to improve osteoporosis diagnosis as miR-30c-2-3p, miR-199a-5p, miR-424-5p, miR-497-5p and miR-877-3p, found in a study by Shuai *et al.*¹⁵ In a study by Verdelli *et al.*, miR-93-5p was identified as able to distinguish between primary osteoporosis and osteoporosis secondary to primary hyperparathyroidism.¹⁶ Moreover, in osteoporosis, a specific miRNA signature was detected in serum and four miRNA clusters had a strong diagnostic potential.¹⁷ Based on these results, a diagnostic kit, OsteomiR®, was developed.

Besides the great effort made in the identification of new diagnostic tools for osteoporosis and sarcopenia, to date, none of such molecular signatures have been associated to muscle wasting in course of post-menopausal osteoporosis in women.

Based on this context, this study aims at identifying a unique and innovative method, based on plasma miRNAs measurement, to predict the skeletal muscle mass decrease in post-menopausal osteoporotic women.

Methods

Study population

In this study, a cohort of post-menopausal osteoporotic women was analysed, as in [18]. With regard to the previous study, a subject was excluded due to sample inadequacy; therefore, 28 post-menopausal osteoporotic women (age range 61.8–85.40 years) were considered. The study cohort was characterized by Caucasian ethnicity, age ≥ 60 years, osteoporosis diagnosed by femur DXA (femoral neck BMD T -score < -2.5) and ability to walk without aids. Exclusion criteria were body mass index (BMI) $> 30 \text{ kg}\cdot\text{m}^{-2}$, estimated glomerular filtration rate (eGFR) $< 60 \text{ mL}\cdot\text{min}^{-1}$, alcohol abuse, active or previous smoke, heart failure, diabetes mellitus, active neoplastic diseases, immunosuppressive treatment including corticosteroids, drugs that alter cognitive function, orthopaedic surgery or fragility fractures in the previous 6 months before the enrolment. All women were free from any anti-osteoporotic treatment, calcium and vitamin D supplementation since at least 6 months prior to the first visit, when osteoporosis diagnosis was made. All participants were characterized for weight (kg), height (m), BMI ($\text{kg}\cdot\text{m}^{-2}$), total fat mass (kg) and appendicular skeletal muscle mass index (ASMMI; $\text{kg}\cdot\text{m}^{-2}$), measured by total-body DXA, and femoral neck BMD T -score values, measured by femur DXA.

DXA examinations were performed on a Hologic QDR-Discovery W densitometer (Hologic Inc., Bedford, MA, USA). Detailed methods for radiological examinations were previously reported in [18].

To highlight the differences between osteoporotic women with different skeletal muscle mass, the overall population was divided in tertiles, based on ASMMI (first tertile: $n = 9$; second tertile: $n = 10$; third tertile: $n = 9$) (Table 1). Based on sarcopenia definition criteria,¹⁹ ASMMI value of $5.5 \text{ kg}\cdot\text{m}^{-2}$ is considered the cut-off for defining sarcopenia in women: an ASMMI value $< 5.5 \text{ kg}\cdot\text{m}^{-2}$ is associated with low skeletal muscle mass and sarcopenia. As ASMMI is a continuous variable that cannot be described by a cut-off-based dichotomy, to investigate better the endophenotypic differences within our cohort, the population was divided in tertiles based on ASMMI. The resulting sub-cohorts were identified by ASMMI values ranging from 4.20 to $5.34 \text{ kg}\cdot\text{m}^{-2}$ (first tertile), $5.44 \text{ kg}\cdot\text{m}^{-2}$ to $6.01 \text{ kg}\cdot\text{m}^{-2}$ (second tertile) and $6.05 \text{ kg}\cdot\text{m}^{-2}$

to $6.69 \text{ kg}\cdot\text{m}^{-2}$ (third tertile). Therefore, we refer to these sub-cohorts as relative-low ASMMI (first tertile), medium-level ASMMI (second tertile) and relative-high ASMMI (third tertile).

In accordance to the Declaration of Helsinki, all subjects were informed about procedures, benefits and possible adverse events associated with the protocol and gave their informed consent. The clinical trial was approved by the ethical committee (Ospedale San Raffaele, Milan, Italy; Ref. No. 17/INT/2017) and registered at clinicaltrials.gov (NCT03382366).

Sample collection

Blood samples were collected from all post-menopausal osteoporotic women considering all pre-analytical variables, in order to obtain the most reliable results.²⁰ Venous blood was collected between 8:00 AM and 10:00 AM from fasting subjects in dipotassium ethylenediaminetetraacetate (K2EDTA) spray-coated tubes (BD Vacutainer®, Becton Dickinson, Milan, Italy) and SST II Advance Vacutainer® (Becton, Dickinson and Co., Franklin Lakes, NJ, USA). Blood samples were then centrifuged at 2000 g for 10 min to get serum and plasma, in the latter case after 15-min homogenization at room temperature (RT). Plasma and serum aliquots were immediately frozen at -80°C until processing.

MicroRNA profiling

Before processing, thawed plasma was centrifuged 5 min at 3000 g. miRNA-enriched total RNA was extracted from each sample and treated with DNase according to miRCURY™ RNA Isolation Kit protocol (Exiqon A/S, Vedbaek, Denmark) and stored at -80°C . miRNA-enriched total RNA was reverse transcribed with miRCURY LNA™ Universal cDNA synthesis kit II and stored at -20°C until assayed. The spike-in UniSp2, UniSp4 and UniSp5 (Exiqon) were added to each sample at the recommended concentration of 2.0, $2.0\cdot 10^{-2}$ and $2.0\cdot 10^{-4} \text{ fmol}\cdot\mu\text{L}^{-1}$, to check the efficiency of RNA extraction, while the spike-in UniSp6 and cel-39-3p (Exiqon) ($1.5\cdot 10^{-1}$ and $2.0\cdot 10^{-3} \text{ fmol}\cdot\mu\text{L}^{-1}$ respectively), to check the efficiency of reverse transcription.

Table 1 Femoral neck T -score, ASMMI and muscle mass of osteoporotic women population divided in tertiles based on ASMMI

	Tertiles			<i>P</i> -value
	1st ($n = 9$)	2nd ($n = 10$) Avg \pm SD	3rd ($n = 9$)	
Femoral neck T -score	-2.82 ± 0.24	-2.72 ± 0.23	-2.70 ± 0.22	0.521
ASMMI ($\text{kg}\cdot\text{m}^{-2}$)	4.88 ± 0.40	5.73 ± 0.23	6.40 ± 0.22	< 0.001
Muscle mass (kg)	11.83 ± 1.203	13.88 ± 1.64	14.59 ± 0.94	< 0.001

Abbreviations: ASMMI, appendicular skeletal muscle mass index; Avg, average; SD, standard deviation.

miRNA expression profile was performed through quantitative real-time polymerase chain reaction (qPCR) using serum/plasma miRCURY LNA™ miRNA focus panel (Exiqon A/S), containing 179 LNA™ primer sets for the most relevant circulating miRNAs, 5 RNA spike-in control primer sets, 2 blank wells and 6 inter-plate calibrators (IPCs). qPCR was carried out on a StepOne Plus instrument (Applied Biosystem, Foster City, CA, USA), using ExiLENT SYBR Green 2X Master Mix (Exiqon). Polymerase activation for 10 min at 95°C was followed by 40 × 10-s amplification cycles at 95°C, 60 s at 60°C and melting curves. Data analysis was performed using GenEx software Version 6 (Exiqon), considering all post-analytical variables.²¹ The quantification cycle (Cq) of the IPC was used to adjust the miRNA Cq values from the qPCR plate runs of each sample. Only miRNAs with an adjusted Cq < 37 were considered for further analysis. The relative expression of analysed miRNAs was calculated by the 2^{-ΔΔCq} method, normalizing on global mean. Haemolysis was checked by the hsa-miR-23a and hsa-miR-451a Cq difference (positive if >7).

miRNA profile analysis was performed dividing the population in tertiles based on ASMMI, comparing miRNA expression levels between the first tertile and the third tertile. Only miRNAs whose expression was ≥ ±1.5-fold and with a *P*-value < 0.05 were considered.

Bioinformatics analysis

Target prediction of ≥ ±1.5-fold either up-regulated or down-regulated miRNAs was performed on miRWalk Version 3.0 (<http://mirwalk.umm.uni-heidelberg.de/>),²² which combines other three target prediction tools (TargetScan, TarBase and miRDB). Only predicted target genes with a score > 0.95, and listed at least by two tools, always considering TarBase, the database of the experimentally validated miRNA–gene interactions, were considered for further bioinformatics analysis. Panther Version 17.0 software was used to perform both gene ontology (GO) enrichment analysis and pathway enrichment analysis (<http://www.pantherdb.org/>). GO analysis was performed classifying predicted target gene into BP, molecular function (MF) and cellular component (CC). Two-sided Fisher's exact test was used and GO and pathway enrichment *P*-values were corrected calculating the false discovery rate (FDR). GO categories and pathways were considered significant when the corrected *P*-value was < 0.05.

Adipo-myokines analysis

Adiponectin and plasminogen activator inhibitor-1 (PAI-1) have been assayed in serum samples through a 2-plex bead-based immunofluorescent assay (Bio-Techne, Minneapolis, MN, USA) by a MagPix™ Luminex System (Bio-Rad Labo-

ratories, Inc., Hercules, CA, USA). Interleukin-8 (IL-8) (Demeditec, Lise-Meitner-Straße, Kiel, Germany) and leptin (Tecan Group Ltd, Männedorf, Switzerland) were assayed in plasma samples of first- and third-tertile osteoporotic women through solid-phase enzyme-linked immunosorbent assay (ELISA). Adiponectin, PAI-1, leptin and IL-8 display a sensitivity of 148, 0.7, 2.13 and 1.1 pg·mL⁻¹, respectively. Assays were performed following the manufacturer's instructions, and all samples were tested in duplicate.

Statistical analysis

The sample size of the entire population was calculated as reported in [18]. In order to define the adequacy of the tertiles-based sub-cohorts division (*n* = 9), a post-hoc power analysis has been performed: Considering an α = 0.05 and an effect size of 1.52, derived from the mean values of ASMMI in the three tertiles (Table 1), 1 – β results 0.99. Differences in femoral neck *T*-score, ASMMI and skeletal muscle mass among the three tertiles were analysed by the Kruskal–Wallis test with Dunn's multiple-comparison test. miRNA expression levels between osteoporotic women of the first tertile and the third tertile were compared through the non-parametric Mann–Whitney test. miRNA diagnostic value was analysed through receiver operating characteristic (ROC) curves. ROC curve-related area under the curve (AUC), sensitivity and sensibility were also calculated.²³ Adipo-myokines circulating levels between osteoporotic women of the first tertile and the third tertile were compared through parametric unpaired *t*-test. All statistic tests were performed considering the distribution of data, calculated with the D'Agostino–Pearson test. Results were considered statistically significant if *P*-values < 0.05. These statistical analyses were performed with Prism® Version 6.01 (GraphPad Software Inc., La Jolla, CA, USA). Univariate and multivariate analyses were performed on R 64 3.5.2. Univariate and multivariate regression models were applied to study the association of miRNAs with clinical parameters as ASMMI, age, BMI, sex, total fat mass, percentage of fat mass, femoral neck *T*-score, fragility fractures and CTx-I, considering all population (first, second and third tertiles).

Data on CTx-I have been published in a previous study on the same population of post-menopausal osteoporotic women by Vitale *et al.*, 2021.¹⁸

Results

Characterization of the study cohort

Twenty-eight osteoporotic women, aged 61.8–85.40 years, were included in the study. Details about the participants are shown in Table 2. Considering the entire population, di-

Table 2 Characterization of the post-menopausal osteoporotic women population

Patients, <i>n</i> = 28	
Sex	
Male	/
Female	28
Age (years)	
(range)	61.80–85.40
Weight (kg)	
(Avg ± SD)	55.58 ± 8.03
Height (m)	
(Avg ± SD)	1.54 ± 0.05
BMI (kg·m ⁻²)	
(Avg ± SD)	23.62 ± 4.05
ASMMI (kg·m ⁻²)	
<5.5	11
>5.5	17
Total fat (kg)	
(Avg ± SD)	20.73 ± 5.72
Femoral neck <i>T</i> -score	
(Avg ± SD)	-2.75 ± 0.23
(range)	[-3.10; -2.50]

Abbreviations: ASMMI, appendicular skeletal muscle mass index; Avg, average; BMI, body mass index; SD, standard deviation.

vided into tertiles based on ASMMI (kg·m⁻²), the three groups significantly differed for skeletal muscle mass (kg) ($P < 0.001$), for ASMMI (kg·m⁻²) ($P < 0.001$), while no differences were observed for femoral neck *T*-score ($P = 0.521$) (Table 1). For miRNAs and adipo-myokines, osteoporotic women included in the first ASMMI tertile and the third tertile were considered.

MicroRNAs profiling and selection

For the comparison of first-to-third ASMMI-based tertiles, fold changes and relative *P*-values of the circulating levels of 179 miRNAs are shown in Table S1. Two miRNAs (hsa-miR-145-5p and hsa-miR-25-3p) were significantly up-regulated, while five (hsa-miR-126-5p, hsa-miR-146a-5p, hsa-miR-221-3p, hsa-miR-374b-5p and hsa-miR-425-5p) were significantly down-regulated in the first tertile compared with the third tertile (Figure 1).

ROC curve analysis was performed for the seven identified miRNAs, to assess their sensitivity and specificity in discriminating between low- and high-ASMMI osteoporotic women: the AUC for the seven miRNAs considered singularly ranged from 0.802 and 1.000 ($P < 0.05$) as shown in Figure 1 and Table 3. Based on Youden's index, sensitivities and specificities were, respectively, 100.00% and 66.67% at a cut-off of 0.242 for hsa-miR-126-5p, 77.78% and 77.78% at a cut-off of 0.291 for hsa-miR-145-5p, 100.00% and 75.00% at a cut-off of 0.250 for hsa-miR-146a-5p, 100.00% and 66.67% at a cut-off of 0.057 for hsa-miR-221-3p, 87.50% and 100.00% at a cut-off of 4.673 for hsa-miR-25-3p, 87.50% and 75.00% at

a cut-off of 0.413 for hsa-miR-374b-5p and 85.71% and 75.00% at a cut-off of 0.263 for hsa-miR-425-5p.

Bioinformatics analysis

Bioinformatics analysis was performed on June 2022. miRWalk Version 3 was used for target prediction analysis: 127 genes were predicted as targets of the 2 up-regulated miRNAs and 66 genes as targets of the 5 down-regulated miRNAs (Tables S2 and S3). Two genes (BCL2L11 and LHFPL2) were expected to be targeted by both up-regulated and down-regulated miRNAs. GO enrichment analysis was performed using Panther to examine the biological functions of target genes. GO analysis has shown 325, 35 and 19 enriched terms in BP, MF and CC, respectively (Figure 2 and Table S4). Thirteen pathways were enriched for all predicted target genes (Figure 3 and Table S4).

Association study between microRNAs and appendicular skeletal muscle mass index

In the analysis described above, the circulating levels of seven miRNAs were identified as differing between the first and third tertiles of ASMMI. However, being ASMMI a continuous variable and distributed over a quite narrow range of ASMMI values in our study population (min: 4.20 kg·m⁻²; max: 6.69 kg·m⁻²), we assessed the relationship of identified miRNA levels with ASMMI, as indexes of skeletal muscle mass.

In particular, five clinical variables were chosen as covariates: age, BMI, fat mass, fat mass percentage and femoral neck *T*-score. All these clinical variables were available for all the 28 participants. In univariate analysis, two miRNAs, hsa-miR-126-5p ($P = 0.007$) and hsa-miR-146a-5p ($P = 0.006$), were significantly associated with ASMMI (Table 4). In bivariate analysis, hsa-miR-126-5p and hsa-miR-25-3p were associated with ASMMI when adjusted for age ($P = 0.042$ and $P = 0.049$, respectively), and hsa-miR-146a-5p when adjusted for age ($P = 0.026$), fat mass percentage ($P = 0.022$) and femoral neck *T*-score ($P = 0.025$) (Table 4). Moreover, association analyses with bone biomarker (CTx-I),¹⁸ fragility fractures and femoral neck *T*-score have not shown any significant association (Table S5).

The combination of hsa-miR-126-5p and hsa-miR-146a-5p gave an AUC of 0.864 ($P = 0.015$), with a sensitivity and a specificity of 77.78% and 100.00%, respectively (Table S6). Each of the other five identified miRNAs was then added to these two miRNA signatures (hsa-miR-126-5p and hsa-miR-146a-5p) in order to investigate any possible improvement in the diagnostic potential. The obtained AUCs ranged from 0.704 to 0.914, with sensitivities and

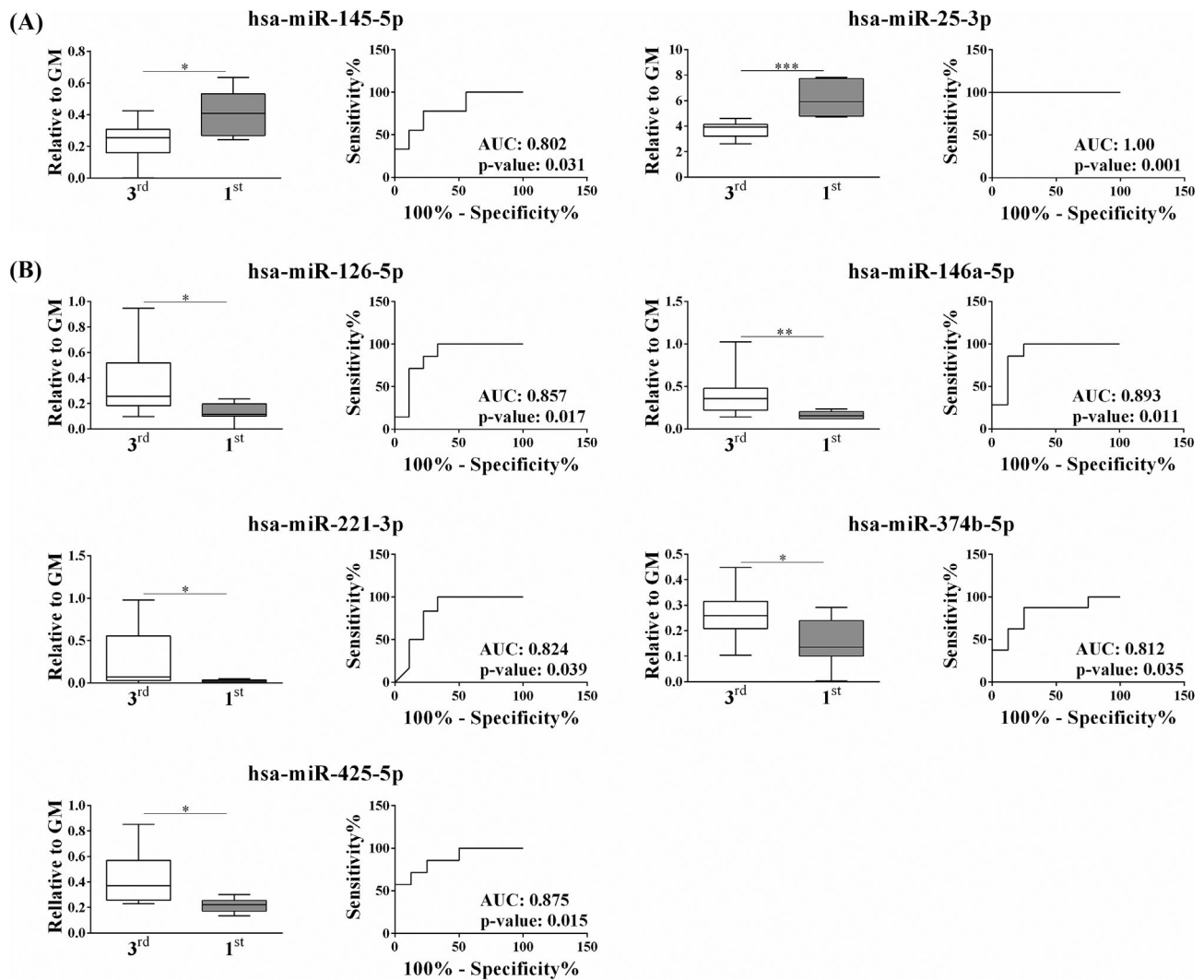


Figure 1 Fold change and receiver operating characteristic (ROC) curve of plasma microRNAs (miRNAs) of post-menopausal osteoporotic women with different skeletal muscle mass. Differences of circulating level and ROC curve analysis of up-regulated miRNAs (A) and down-regulated miRNAs (B) in osteoporotic women within the first tertile (relative-low appendicular skeletal muscle mass index [ASMMI]) compared with osteoporotic women within the third tertile (relative-high ASMMI). Circulating levels of miRNAs are expressed as min to max and compared using a Mann–Whitney *t*-test. The relative area under the curve (AUC) and *P*-value are shown for each ROC curve analysis. The statistics were considered significant when *P* < 0.05 (**P* < 0.05, ***P* < 0.01 and ****P* < 0.001). Statistical analysis was performed with Prism® Version 6.01 (GraphPad Software).

Table 3 AUC, sensitivity and specificity of seven identified miRNAs in osteoporotic women

miRNA	AUC [95% CI]	<i>P</i> -value	Youden's index	Cut-off	Sensitivity (%)	Specificity (%)
hsa-miR-145-5p	0.802 [0.596–1.009]	0.031	0.556	>0.291	77.78	77.78
hsa-miR-25-3p	1.000 [1.000–1.000]	0.001	1.00	>4.673	100.00	100.00
hsa-miR-126-5p	0.857 [0.660–1.054]	0.017	0.667	<0.242	100.00	66.67
hsa-miR-146a-5p	0.893 [0.713–1.072]	0.011	0.750	<0.250	100.00	75.00
hsa-miR-221-3p	0.824 [0.603–1.045]	0.039	0.667	<0.0573	100.00	66.67
hsa-miR-374b-5p	0.812 [0.592–1.033]	0.036	0.625	<0.413	87.50	75.00
hsa-miR-425-5p	0.875 [0.697–1.053]	0.015	0.607	<0.263	85.71	75.00

Abbreviations: AUC, area under the curve; CI, confidence interval; miRNAs, microRNAs.

specificities ranging from 55.56% to 88.89% and from 66.67% to 100.00%, respectively, as shown in *Table S6*. The highest AUC was obtained for the combinations hsa-miR-126-5p, hsa-miR-146a-5p and hsa-miR-425-5p

(AUC = 0.914; sensitivity = 77.78%; specificity = 100.00%) and hsa-miR-126-5p, hsa-miR-146a-5p, hsa-miR-145-5p and hsa-miR-25-3p (AUC = 0.901; sensitivity = 88.89%; specificity = 100.00%).

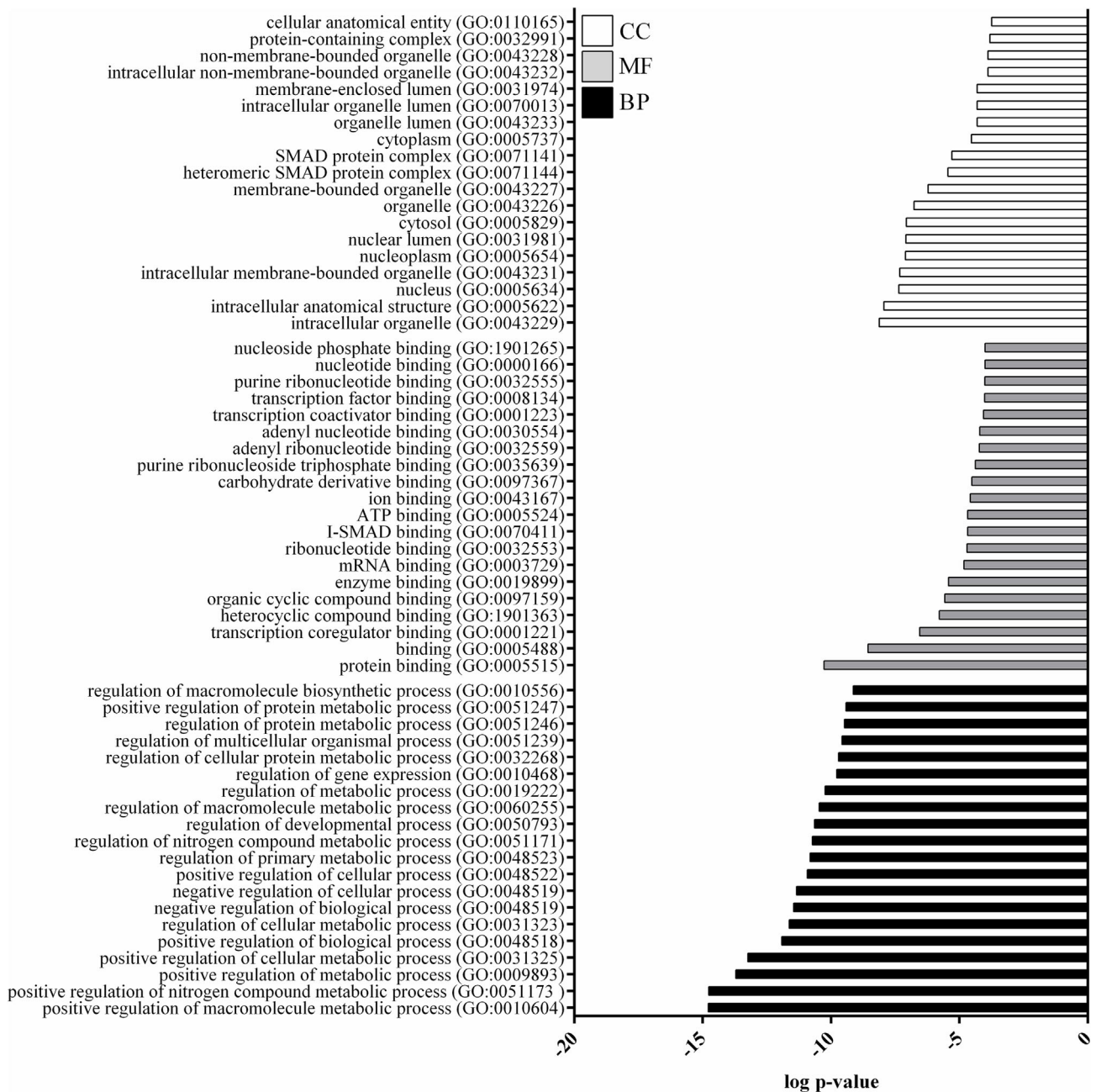


Figure 2 Gene ontology (GO) of target genes predicted for up-regulated and down-regulated microRNAs differently expressed in post-menopausal osteoporotic women with different skeletal muscle mass. GO has classified target genes in cellular component (CC), molecular function (MF) and biological process (BP). The most enriched categories (maximum 20) are shown. GO was performed with Panther Version 17.0 (<http://www.pantherdb.org/>), and the related statistic is shown in *Table S4*.

Adipo-myokines analysis

Circulating levels of adipokines (adiponectin, leptin and PAI-1) and myokines (IL-8), involved in the definition of the metabolic inflammatory environment that supports the age-associated muscle mass wasting, were evaluated in this

study cohort. None of these mediators significantly differed in the study cohort between the first and third tertiles of ASMMI. However, adiponectin and IL-8 showed a trend to the increase in the first tertile compared with the third tertile while PAI-1 and leptin showed a trend to decrease (*Figure 4*).

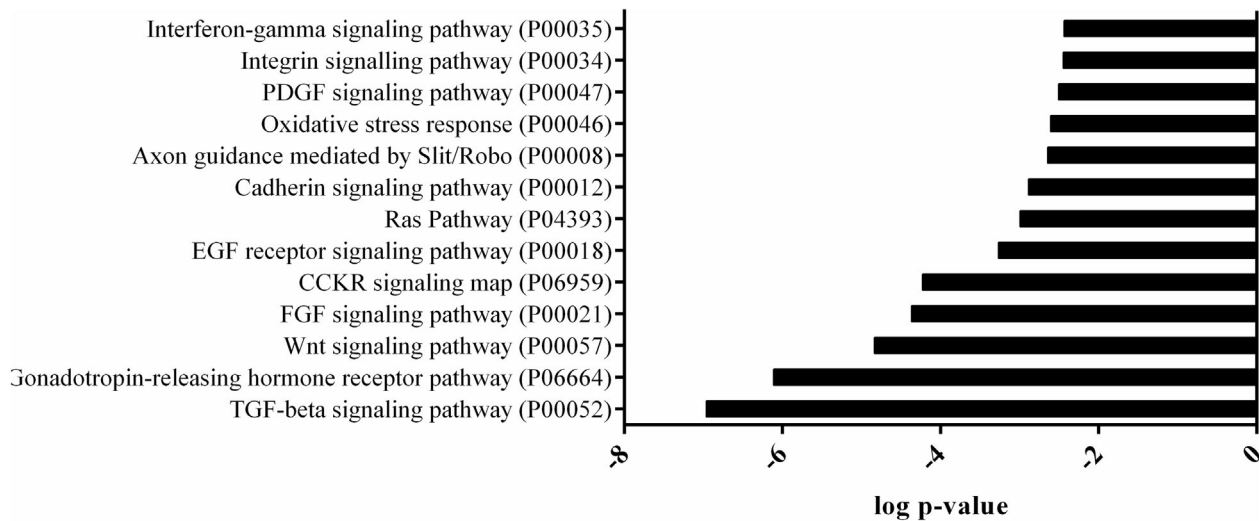


Figure 3 Pathway enrichment analysis of predicted target genes predicted for up-regulated and down-regulated microRNAs (miRNAs) differently expressed in post-menopausal osteoporotic women with different skeletal muscle mass. Analysis of the pathway enriched for target genes of the up-regulated and down-regulated miRNAs in osteoporotic women of first tertile (relative-low appendicular skeletal muscle mass index [ASMMI]) compared with osteoporotic women of third tertile (relative-high ASMMI). All the enriched pathways are shown. The analysis was performed using Panther Version 17.0 (<http://www.pantherdb.org/>), and the related statistic is shown in *Table S4*.

Discussion

Osteoporosis and sarcopenia are age-related disorders, almost invariably coexisting, characterized, respectively, by loss of BMD and skeletal muscle mass. The resulting net clinical outcome is the increased risk of fall and fractures that may lead to physical disability, poor quality of life and increased mortality risk.^{1,2} The progressive aging of the population brings to the increase of the prevalence of muscle skeletal disorders, and, therefore, novel diagnostic tools are needed for their diagnosis and monitoring, in order to reduce the incidence of fractures. Our study was aimed at identifying a specific miRNA signature, in plasma, able to predict the skeletal muscle mass in post-menopausal osteoporotic women. Several studies attempted at identifying circulating miRNAs associated with osteoporosis or sarcopenia, with the final aim to provide new biomarkers to be implemented into clinical practice for a more accurate diagnosis.^{15,17,24} Although it has been widely established that alteration of circulating miRNA levels is associated with BMD and decline of skeletal muscle mass during aging, very little is known about circulating miRNA signatures that describe the coexistence of both disorders. Therefore, to our knowledge, this study is the first in this context. The expression level of a panel of miRNA was assessed in the plasma of 28 women affected by primary osteoporosis. ASMMI was used as the index of skeletal muscle mass, with a value of ASMMI < 5.5 kg·m⁻² being considered associated with sarcopenia.¹⁹ In order to avoid a cut-off-based dichotomy of the population, to investigate better the endophenotypic differences within our real-life-like cohort, the population was divided in tertiles based on ASMMI. The resulting sub-cohorts were identified by ASMMI values

ranging from 4.20 to 5.34 kg·m⁻² (first tertile), 5.44 to 6.01 kg·m⁻² (second tertile) and 6.05 to 6.69 kg·m⁻² (third tertile). In these three newly generated groups, BMD values, as indicated by the femoral neck *T*-score, were homogeneously distributed, while differences were, of course, found for ASMMI and BMI. Seven miRNAs were found ≥ 1.5 up-regulated or down-regulated in the first tertile compared with third tertile. More specifically, hsa-miR-145-5p and hsa-miR-25-3p were up-regulated while hsa-miR-126-5p, hsa-miR-146a-5p, hsa-miR-221-3p, hsa-miR-374b-5p and hsa-miR-425-5p were down-regulated. Recent studies identified an association between circulating miR-126, miR-146a and miR-221 and skeletal muscle mass in aging and sarcopenia; however, their potential as biomarkers in sarcopenia is controversial. Similarly to what observed in our study, Liu and colleagues found the plasma level of miR-146a decreased in sarcopenic subjects compared with normal and dynapenic subjects and associated with skeletal muscle mass.²⁵ Differently from our results, in a study by He and colleagues that analysed the circulating level of miRNAs associated with skeletal and cardiac muscle, angiogenesis or inflammation in normal and sarcopenic subjects, the plasma levels of miR-126, miR-146a and miR-221 did not differ between the two groups.¹⁴ By contrast, our results from ROC curve analysis have confirmed the potential applicability of the seven identified miRNAs as biomarkers of skeletal muscle wasting. The diagnostic performance of these miRNAs showed that for all seven miRNAs, AUC value was >0.8, thus exceeding the appropriateness cut-off of AUC > 0.7, indicated by Swets.²³

Subsequent *in silico* analyses predicted 127 and 66 target genes, for up-regulated and down-regulated miRNAs, respectively, involved in crucial pathways associated to senescence

Table 4 Association analysis of the identified miRNAs with ASMMI

miRNA	Estimate (SE)	P-value	Estimate (SE)	P-value	Estimate (SE)	P-value	Estimate (SE)	P-value	Estimate (SE)	P-value	Estimate (SE)	P-value
	Age adjusted		BMI adjusted		Fat adjusted		%Fat adjusted		Femoral neck T-score adjusted			
hsa-miR-221-3p	0.15 (0.11)	0.189	0.15 (0.11)	0.187	0.10 (0.15)	0.497	0.13 (0.12)	0.292	0.13 (0.10)	0.226	0.13 (0.11)	0.275
hsa-miR-374b-5p	0.07 (0.04)	0.085	0.07 (0.00)	0.051	0.04 (0.05)	0.399	0.06 (0.04)	0.152	0.06 (0.04)	0.089	0.06 (0.04)	0.117
hsa-miR-145-5p	-0.06 (0.13)	0.671	-0.06 (0.13)	0.645	-0.11 (0.17)	0.532	-0.13 (0.13)	0.353	-0.06 (0.13)	0.652	-0.04 (0.13)	0.763
hsa-miR-25-3p	-1.08 (0.53)	0.051	-1.11 (0.53)	0.049	-0.82 (0.67)	0.233	-0.99 (0.56)	0.088	-1.07 (0.53)	0.057	-1.08 (0.54)	0.057
hsa-mi-146a-5p	0.14 (0.06)	0.021	0.14 (0.06)	0.026	0.04 (0.07)	0.531	0.12 (0.06)	0.063	0.14 (0.06)	0.022	0.14 (0.06)	0.025
hsa-miR-126-5p	0.15 (0.07)	0.049	0.14 (0.07)	0.042	0.08 (0.09)	0.379	0.12 (0.08)	0.132	0.15 (0.07)	0.056	0.13 (0.07)	0.077
hsa-miR-425-5p	0.12 (0.06)	0.066	0.12 (0.06)	0.071	0.14 (0.08)	0.107	0.14 (0.07)	0.054	0.14 (0.07)	0.054	0.11 (0.06)	0.088

Note: Statistically significant associations are reported in bold.

Abbreviations: ASMMI, appendicular skeletal muscle mass index; BMI, body mass index; miRNAs, microRNAs.

in skeletal muscle. Among the 13 enriched pathways, those involving transforming growth factor (TGF) β , Wnt, fibroblast growth factor (FGF) and cadherin are known to have a role in skeletal muscle homeostasis, maintenance and regeneration. TGF β is involved in skeletal muscle regeneration. After skeletal muscle damage, the level of TGF β increases, inducing a transient inflammatory response to promote regeneration. An increasing inflammatory status, coupled with the increase of TGF β , promotes the transition of skeletal muscle to fibrotic tissue.²⁶ Being involved in muscle repair, Wnt signalling activation resulted impaired in the aged skeletal muscle; particularly, the imbalance of Wnt and Notch signalling pathways leads to the age-related decrease in muscle regenerative capacity.²⁷ Wnt pathway is also strictly connected to cadherin signalling pathway: In C2C12 cell line, it was demonstrated that M-cadherin regulates β -catenin phosphorylation and, consequently, the Wnt cascade and, thus, affects myogenesis.²⁸ FGF signalling pathway is essential for skeletal muscle stem cells and its deregulation could lead to decrease of stem cell self-renewal and, consequently, muscle wasting.²⁹

Four predicted target genes might be involved in oxidative stress response. Reactive oxygen species (ROS) accumulation, a phenomenon that takes place during aging due to the impaired mitochondrial activity, affects skeletal muscle throughout the nuclear factor κ B (NF- κ B)-dependent inhibition of myogenesis, impaired sensitivity to Ca²⁺, contractile function and strength, and satellite cells activity, leading to limited regenerative potential.³⁰

Noteworthy, the expression of some of the seven miRNAs identified in this study has been shown to be altered in skeletal muscle during aging in human and mice or has been shown involved in skeletal muscle development. In a study by Rivas and colleagues, hsa-miR-126 was found differentially expressed in skeletal muscle of old males compared with healthy young males. Bioinformatics analysis and subsequent functional in vitro analysis, on murine myoblasts, revealed the role of miR-126 in skeletal muscle growth and in the activation of IGF-1 signalling.³¹ Moreover, hsa-miR-126, which is predominantly expressed in endothelial cells and is involved in angiogenesis and inflammation, has been shown regulated by exercise, and several studies demonstrated that exercise increases its circulating levels in healthy individuals.³² It was also demonstrated that hsa-miR-126 is involved in the regulation of smooth muscle cells turnover.³³

hsa-miR-146a was found down-regulated in gastrocnemius muscles of 24-month-old mice compared with 6-month-old mice.³⁴ In another study, in vivo and in vitro experiments showed that hsa-miR-146a-5p is involved in muscle fibrosis progression via TGF β /Smad4 signalling. It was demonstrated that miR-146a-5p expression is reduced both in a fibrotic mouse model and in C2C12 myotubes treated with TGF β .³⁵

miR-145a-5p is another miRNA involved in myogenesis regulation. Du et al. demonstrated that miR-145-5p, up-regu-

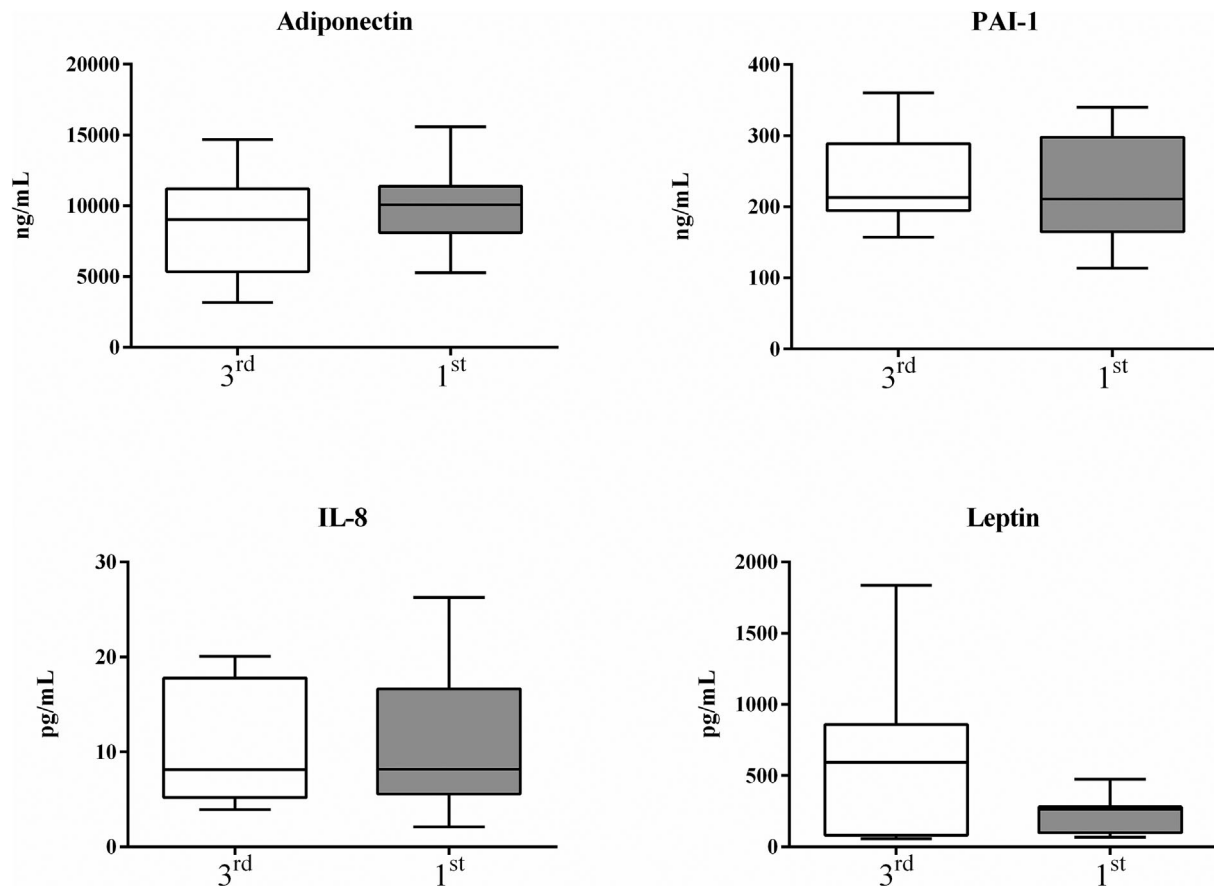


Figure 4 Adipo-myokines plasma profile in post-menopausal osteoporotic women with different skeletal muscle mass. Differences in circulating levels of adipo-myokines in osteoporotic women of first tertile (relative-low appendicular skeletal muscle mass index [ASMMI]) compared with osteoporotic women of third tertile (relative-high ASMMI). All data are expressed as min to max and compared through a parametric unpaired *t*-test. Statistical analysis was performed with Prism® Version 6.01 (GraphPad Software). The differences were considered significant when $P < 0.05$ (* $P < 0.05$, ** $P < 0.01$ and *** $P < 0.001$). IL-8, interleukin-8; PAI-1, plasminogen activator inhibitor-1.

lated during C2C12 differentiation, promotes myoblast differentiation by enhancing the expression of Wnt signalling pathway-related gene.³⁶

Several studies have identified miR-221 as associated with aging muscle wasting. In a study by Hamrick et al., miR-221 was found down-regulated in skeletal muscle of 24-month-old mice, with reduced skeletal muscle mass and size, compared with 12-month-old mice,³⁷ while, in a study by McCarthy et al., miR-221 was associated with age-related muscle atrophy; in this study, the expression of 18 miRNAs, including miR-221, was altered in rat soleus after 2 or 7 days of hind limb suspension, compared with normal soleus muscle.³⁸ In human, hsa-miR-221-3p was found decreased in circulation and increased in muscle biopsies in active healthy males who underwent high aerobic exercise-induced energy expenditure.³⁹

In a microarray-based study by Drummond et al., on skeletal muscle biopsies from young and old males, miR-25 was found up-regulated in skeletal muscle samples of older individuals.⁴⁰

Also, miR-374b is involved in myoblast differentiation. In a study by Ma et al., miR-374 was demonstrated to inhibit C2C12 cells differentiation by directly inhibiting Myf6 gene expression.⁴¹ hsa-miR-374b-5p was also found down-regulated in patients with sporadic amyotrophic lateral sclerosis, a neurodegenerative condition characterized by loss of motor neurons and progressive muscle wasting, compared with healthy controls.⁴²

Finally, a recent study, by Agostini et al., found that hsa-miR-425-5p is significantly up-regulated in serum of sarcopenic patients after 30 days of rehabilitative treatment.⁴³

Considering that, in our results, hsa-miR-126-5p and hsa-miR-146a-5p were significantly associated with ASMMI, their combination further increased the AUC value, and therefore, their diagnostic potential, compared with the single miRNAs AUC. Furthermore, the completion of the molecular signature with either hsa-miR-425-5p or the pair hsa-miR-145-5p and hsa-miR-25-3p performed even better.

Finally, aging is characterized by a chronic low-grade inflammation and by several changes in body composition, par-

ticularly in adipose tissue, as in skeletal muscle mass and bone, leading to changes in circulating levels of inflammatory cytokines, adipokines and myokines.⁴⁴ Serum levels of adiponectin and PAI-1 and plasma levels of leptin and IL-8 were assayed to investigate the crosstalk between skeletal muscle and adipose tissue; however, no differences in circulating level of these cytokines were observed between post-menopausal osteoporotic women with low and high skeletal muscle mass.

Although this study represents a first approach to the identification of a miRNA-based signature that describes both skeletal muscle mass and BMD decline in elderly women, it has some limitation. First, the endpoint of this study focused on skeletal muscle mass (by the mean of ASMMI); however, according with the definition of sarcopenia given by the European Working Group on Sarcopenia in Older People (EWGSOP) and the International Working Group on Sarcopenia (IWGS), diagnosis of sarcopenia also includes the measurement of muscle function and strength.^{2,19} Therefore, the molecular signature we identified defines the changes in muscle mass, in post-menopausal osteoporotic women, but their application to the diagnosis of sarcopenia should be assayed and validated. The validation of the identified miRNAs will be performed on a large cohort of post-menopausal osteoporotic women and considering a control group of healthy women (no menopause women without osteoporosis and with normal skeletal muscle mass). Moreover, the biological function of the identified miRNAs, defined throughout the bioinformatics, will need an experimental validation in order to highlight the mechanistic role of these miRNAs in skeletal muscle physiology.

References

1. NIH Consensus Development Panel on Osteoporosis Prevention D, Therapy. Osteoporosis prevention, diagnosis, and therapy. *JAMA* 2001;**285**:785–795.
2. Fielding RA, Vellas B, Evans WJ, Bhasin S, Morley JE, Newman AB, et al. Sarcopenia: an undiagnosed condition in older adults. Current consensus definition: prevalence, etiology, and consequences. International Working Group on Sarcopenia. *J Am Med Dir Assoc* 2011;**12**:249–256.
3. Hirschfeld HP, Kinsella R, Duque G. Osteosarcopenia: where bone, muscle, and fat collide. *Osteoporos Int* 2017;**28**:2781–2790.
4. Assessment of fracture risk and its application to screening for postmenopausal osteoporosis. Report of a WHO Study Group. *World Health Organ Tech Rep Ser* 1994;**843**:1–129.
5. Fuggle N, Shaw S, Dennison E, Cooper C. Sarcopenia. *Best Pract Res Clin Rheumatol* 2017;**31**:218–242.
6. Kanis JA, Harvey NC, Johansson H, Oden A, Leslie WD, McCloskey EV. FRAX and fracture prediction without bone mineral density. *Climacteric* 2015;**18**:2–9.
7. Malmstrom TK, Miller DK, Simonsick EM, Ferrucci L, Morley JE. SARC-F: a symptom score to predict persons with sarcopenia at risk for poor functional outcomes. *J Cachexia Sarcopenia Muscle* 2016;**7**:28–36.
8. Fathi M, Heshmat R, Ebrahimi M, Salimzadeh A, Ostovar A, Fathi A, et al. Association between biomarkers of bone health and osteosarcopenia among Iranian older people: the Bushehr Elderly Health (BEH) program. *BMC Geriatr* 2021;**21**:654.
9. Poggiongalle E, Cherry KE, Su LJ, Kim S, Myers L, Welsh DA, et al. Body composition, IGF1 status, and physical functionality in nonagenarians: implications for osteosarcopenia. *J Am Med Dir Assoc* 2019;**20**:70–75.e2.
10. Ha M, Kim VN. Regulation of microRNA biogenesis. *Nat Rev Mol Cell Biol* 2014;**15**:509–524.
11. Brzeszczynska J, Brzeszczynski F, Hamilton DF, McGregor R, Simpson A. Role of microRNA in muscle regeneration and diseases related to muscle dysfunction in atrophy, cachexia, osteoporosis, and osteoarthritis. *Bone Jt Res* 2020;**9**:798–807.
12. Condrat CE, Thompson DC, Barbu MG, Bugnar OL, Boboc A, Cretoiu D, et al. miRNAs as biomarkers in disease: latest findings regarding their role in diagnosis and prognosis. *Cells-Basel* 2020;**9**:276.
13. Bottani M, Banfi G, Lombardi G. The clinical potential of circulating miRNAs as biomarkers: present and future applications for diagnosis and prognosis of age-associated bone diseases. *Biomolecules* 2020;**10**:589.
14. He N, Zhang YL, Zhang Y, Feng B, Zheng Z, Wang D, et al. Circulating microRNAs in plasma decrease in response to sarcopenia in the elderly. *Front Genet* 2020;**11**:167.
15. Shuai Y, Liao L, Su X, Sha N, Li X, Wu Y, et al. Circulating microRNAs in serum as novel biomarkers for osteoporosis: a case-control study. *Ther Adv Musculoskelet Dis* 2020;**12**:1759720X20953331.
16. Verdelli C, Sansoni V, Perego S, Favero V, Vitale J, Terrasi A, et al. Circulating

Acknowledgements

The authors would like to thank all the participants in the study.

Open access funding provided by BIBLIOSAN.

Open access funding provided by BIBLIOSAN.

Conflict of interest statement

The authors declare that the research was conducted in the absence of any commercial or financial relationships that could be construed as a potential conflict of interest.

Data availability statement

The dataset supporting the conclusions of this article is available in the Zenodo repository (<https://zenodo.org/record/7541454#.Y8aZsn3MKUK>).

Online supplementary material

Additional supporting information may be found online in the Supporting Information section at the end of the article.

- fractures-related microRNAs distinguish primary hyperparathyroidism-related from estrogen withdrawal-related osteoporosis in postmenopausal osteoporotic women: a pilot study. *Bone* 2020;**137**:115350.
17. Kerschman-Schindl K, Hackl M, Boschitsch E, Foger-Samwald U, Nagele O, Skalicky S, et al. Diagnostic performance of a panel of miRNAs (OsteomiR) for osteoporosis in a cohort of postmenopausal women. *Calcif Tissue Int* 2021;**108**:725–737.
 18. Vitale JA, Sansoni V, Faraldi M, Messina C, Verdelli C, Lombardi G, et al. Circulating carboxylated osteocalcin correlates with skeletal muscle mass and risk of fall in postmenopausal osteoporotic women. *Front Endocrinol* 2021;**12**:669704.
 19. Cruz-Jentoft AJ, Bahat G, Bauer J, Boirie Y, Bruyere O, Cederholm T, et al. Sarcopenia: revised European consensus on definition and diagnosis. *Age Ageing* 2019;**48**:601.
 20. Faraldi M, Sansoni V, Perego S, Gomasasca M, Kortas J, Ziemann E, et al. Study of the preanalytical variables affecting the measurement of clinically relevant free-circulating microRNAs: focus on sample matrix, platelet depletion, and storage conditions. *Biochem Med* 2020;**30**:010703.
 21. Faraldi M, Gomasasca M, Sansoni V, Perego S, Banfi G, Lombardi G. Normalization strategies differently affect circulating miRNA profile associated with the training status. *Sci Rep* 2019;**9**:1584.
 22. Sticht C, De La Torre C, Parveen A, Gretz N. miRWalk: an online resource for prediction of microRNA binding sites. *PLoS ONE* 2018;**13**:e0206239.
 23. Swets JA. Measuring the accuracy of diagnostic systems. *Science* 1988;**240**:1285–1293.
 24. Jung HJ, Lee KP, Kwon KS, Suh Y. MicroRNAs in skeletal muscle aging: current issues and perspectives. *J Gerontol A Biol Sci Med Sci* 2019;**74**:1008–1014.
 25. Liu HC, Han DS, Hsu CC, Wang JS. Circulating MicroRNA-486 and MicroRNA-146a serve as potential biomarkers of sarcopenia in the older adults. *BMC Geriatr* 2021;**21**:86.
 26. Burks TN, Cohn RD. Role of TGF- β signaling in inherited and acquired myopathies. *Skelet Muscle* 2011;**1**:19.
 27. Arthur ST, Cooley ID. The effect of physiological stimuli on sarcopenia; impact of Notch and Wnt signaling on impaired aged skeletal muscle repair. *Int J Biol Sci* 2012;**8**:731–760.
 28. Wang Y, Mohamed JS, Alway SE. M-cadherin-inhibited phosphorylation of β -catenin augments differentiation of mouse myoblasts. *Cell Tissue Res* 2013;**351**:183–200.
 29. Pawlikowski B, Vogler TO, Gadek K, Olwin BB. Regulation of skeletal muscle stem cells by fibroblast growth factors. *Dev Dyn* 2017;**246**:359–367.
 30. Lian D, Chen MM, Wu H, Deng S, Hu X. The role of oxidative stress in skeletal muscle myogenesis and muscle disease. *Antioxidants* 2022;**11**:755.
 31. Rivas DA, Lessard SJ, Rice NP, Lustgarten MS, So K, Goodyear LJ, et al. Diminished skeletal muscle microRNA expression with aging is associated with attenuated muscle plasticity and inhibition of IGF-1 signaling. *FASEB J* 2014;**28**:4133–4147.
 32. Ma Y, Liu H, Wang Y, Xuan J, Gao X, Ding H, et al. Roles of physical exercise-induced MiR-126 in cardiovascular health of type 2 diabetes. *Diabetol Metab Syndr* 2022;**14**:169.
 33. Zhou J, Li YS, Nguyen P, Wang KC, Weiss A, Kuo YC, et al. Regulation of vascular smooth muscle cell turnover by endothelial cell-secreted microRNA-126: role of shear stress. *Circ Res* 2013;**113**:40–51.
 34. Kim JY, Park YK, Lee KP, Lee SM, Kang TW, Kim HJ, et al. Genome-wide profiling of the microRNA-mRNA regulatory network in skeletal muscle with aging. *Aging* 2014;**6**:524–544.
 35. Sun Y, Li Y, Wang H, Li H, Liu S, Chen J, et al. miR-146a-5p acts as a negative regulator of TGF- β signaling in skeletal muscle after acute contusion. *Acta Biochim Biophys Sin* 2017;**49**:628–634.
 36. Du J, Li Q, Shen L, Lei H, Luo J, Liu Y, et al. miR-145a-5p promotes myoblast differentiation. *Biomed Res Int* 2016;**2016**:5276271.
 37. Hamrick MW, Herberg S, Arounleut P, He HZ, Shiver A, Qi RQ, et al. The adipokine leptin increases skeletal muscle mass and significantly alters skeletal muscle miRNA expression profile in aged mice. *Biochem Biophys Res Commun* 2010;**400**:379–383.
 38. McCarthy JJ, Esser KA, Peterson CA, Dupont-Versteegden EE. Evidence of MyomiR network regulation of β -myosin heavy chain gene expression during skeletal muscle atrophy. *Physiol Genomics* 2009;**39**:219–226.
 39. Margolis LM, Hatch-McChesney A, Allen JT, DiBella MN, Carrigan CT, Murphy NE, et al. Circulating and skeletal muscle microRNA profiles are more sensitive to sustained aerobic exercise than energy balance in males. *J Physiol* 2022;**600**:3951–3963.
 40. Drummond MJ, McCarthy JJ, Sinha M, Spratt HM, Volpi E, Esser KA, et al. Aging and microRNA expression in human skeletal muscle: a microarray and bioinformatics analysis. *Physiol Genomics* 2011;**43**:595–603.
 41. Ma Z, Sun X, Xu D, Xiong Y, Zuo B. MicroRNA, miR-374b, directly targets Myf6 and negatively regulates C2C12 myoblasts differentiation. *Biochem Biophys Res Commun* 2015;**467**:670–675.
 42. Waller R, Goodall EF, Milo M, Cooper-Knock J, Da Costa M, Hobson E, et al. Serum miRNAs miR-206, 143-3p and 374b-5p as potential biomarkers for amyotrophic lateral sclerosis (ALS). *Neurobiol Aging* 2017;**55**:123–131.
 43. Agostini S, Mancuso R, Costa AS, Guerini FR, Trecate F, Miglioli R, et al. Sarcopenia associates with SNAP-25 SNPs and a miRNAs profile which is modulated by structured rehabilitation treatment. *J Transl Med* 2021;**19**:315.
 44. Gomasasca M, Banfi G, Lombardi G. Myokines: the endocrine coupling of skeletal muscle and bone. *Adv Clin Chem* 2020;**94**:155–218.